Cellular and Molecular Life Sciences (2023) 80:159
https://doi.org/10.1007/s00018-023-04802-y



ORIGINAL ARTICLE

# Excessive iron inhibits insulin secretion via perturbing transcriptional regulation of *SYT7* by OGG1

Xingqi Zhao[1] · Ying Ma[1] · Munan Shi[1] · Miaoling Huang[1] · Jingyu Xin[1] · Shusheng Ci[2] · Meimei Chen[3] · Tao Jiang[4] · Zhigang Hu[1] · Lingfeng He[1] · Feiyan Pan[1] · Zhigang Guo[1]

Received: 1 January 2023 / Revised: 8 May 2023 / Accepted: 8 May 2023 / Published online: 20 May 2023


## Abstract

Although iron overload is closely related to the occurrence of type 2 diabetes mellitus (T2DM), the specific mechanism is unclear. Here, we found that excessive iron inhibited the secretion of insulin (INS) and impaired islet β cell function through downregulating *Synaptotagmin 7* (*SYT7*) in iron overload model in vivo and in vitro. Our results further demonstrated that 8-oxoguanine DNA glycosylase (OGG1), a key protein in the DNA base excision repair, was an upstream regulator of *SYT7*. Interestingly, such regulation could be suppressed by excessive iron. *Ogg1*-null mice, iron overload mice and *db/db* mice exhibit reduced INS secretion, weakened β cell function and subsequently impaired glucose tolerance. Notably, SYT7 overexpression could rescue these phenotypes. Our data revealed an intrinsic mechanism by which excessive iron inhibits INS secretion through perturbing the transcriptional regulation of *SYT7* by OGG1, which suggested that SYT7 was a potential target in clinical therapy for T2DM.

**Keywords** Vesicle transport · Gene transcription · Oxidative stress · Chronic degenerative disease · Target therapy

## Introduction

T2DM is a chronic metabolic disorder due to declining β cell function, and usually accompanied by a reduced sensitivity to INS [1]. This disease is fueled by interactions between multiple susceptible genetic loci and various environmental and behavioral factors [2]. Recently it has been shown that excessive iron intake and improper use of iron supplements are closely related to the occurrence of T2DM [3]. The serum iron level of T2DM patients is higher than that of the health [4]. Until now, the causal relationship between excessive iron and β cell dysfunction and the underlying mechanism are not yet fully understood.

Oxidative stress is considered to be responsible for iron overload-induced islet β cell dysfunction as excessive iron can lead to peroxidation through the Fenton reaction [5]. In living cells, the peroxidation environment can easily cause the oxidative modification of G in genomic DNA to 7,8-dihydro-8-oxoguanine (8-oxoG) due to the low redox potential of guanine. OGG1, a key protein for the response to oxidative stress, binds and excises oxidized 8-oxoG in the genome to maintain the stability of the genome [6]. Mutation of OGG1 has been implicated in the development of certain diseases, including Alzheimer's disease [7], atherosclerosis, cancer and diabetes [8, 9]. Although *Ogg1* knockout ($Ogg1^{-/-}$) mice exhibit normal development, they tend to show the characteristics of metabolic syndrome, such as impaired glucose tolerance [10]. To date, there is no clear mechanistic explanation of OGG1 function in metabolism. Recent evidence suggests that in addition to the classic DNA repair function [6], OGG1 is also involved in the

Feiyan Pan: Lead contact.

✉ Feiyan Pan
panfeiyan@njnu.edu.cn

✉ Zhigang Guo
guo@njnu.edu.cn

1 Jiangsu Key Laboratory for Molecular and Medical Biotechnology, College of Life Sciences, Nanjing Normal University, 1 WenYuan Road, Nanjing 210023, China

2 School of Basic Medical Sciences, Nanjing Medical University, Nanjing 211166, Jiangsu, China

3 Department of Endocrinology, The Second Affiliated Hospital of Nanjing University of Chinese Medicine, Nanjing 210000, Jiangsu, China

4 Department of Geriatrics, The Second Affiliated Hospital of Nanjing University of Chinese Medicine, Nanjing 210000, Jiangsu, China

transcriptional regulation of several genes, such as *TNFα* [11], *HRAS* [12], *VEGF* [13] and *c-Myc* [14]. The identification of a new downstream target of OGG1 may shed light on its role in metabolic processes.

In this study, we focused on the effect and mechanism of iron overload on islet β cell dysfunction and found that excessive iron impaired INS secretion via decreasing the expression of SYT7, a key molecule in this process. We further identified that *SYT7* was a new downstream factor regulated by OGG1 and such regulation could be perturbed by excessive iron. Together, this novel finding revealed a hitherto unknown mechanism by which excessive iron inhibited INS secretion via perturbing the transcription regulation of *SYT7* by OGG1, and therefore impaired islet β cell function.

## Materials and methods

### Mouse model

All animal experiments in this study were carried out in strict accordance with the guidance scheme formulated by the ethical review committee of experimental animal welfare of Nanjing Normal University (Approval No. IACUC-20200515). Male C57BL/6J mice, male *db/db* mice (C57BLKS/JNju background), and female and male $Ogg1^{+/-}$ mice (C57BL/6J background) were purchased from GemPharmatech Co., Ltd. (N000013, T002407, T014260, Nanjing, China) and raised in the experimental animal center of Nanjing Normal University. The feeding conditions were 12 h of light/12 h of dark cycle, ambient temperature of 24°C, relative humidity of 50%, and freely available drinking water. $Ogg1^{+/+}$ and $Ogg1^{-/-}$ mice were obtained from $Ogg1^{+/-}$ mice. According to the instructions corresponding to Article No. T014260, the mouse genotype was identified by PCR. CRISPR/Cas9 technology was used for the knockout of this gene.

$Fe^{2+}$ mice were obtained by feeding 4-week-old male C57BL/6J mice with $FeSO_4$ compound diet (according to the time for feeding like 1 month, 2 months, 3 months and 4 months, recorded as $Fe^{2+}$-1m, $Fe^{2+}$-2m, $Fe^{2+}$-3m and $Fe^{2+}$-4m respectively). The sibling mice fed on common diet (MD17121, provided by Jiangsu Mediscience Biomedical Co., Ltd.) were used as control (CW mice, CW-1m, CW-2m, CW-3m and CW-4m were recorded according to feeding for 1 month, 2 months, 3 months and 4 months respectively). The $FeSO_4$ compound feeding is a kind of common diet with an additional 21.5 g/kg of $FeSO_4{\cdot}7H_2O$ (Jiangsu XieTong Bioengineering Co., Ltd.).

In the rescue experiment of $Ogg1^{-/-}$ mice, the initial injection time of adeno-associated virus serotype 8 vector (AAV8)-null/SYT7 was 3 weeks old. In the rescue experiment of $Fe^{2+}$ mice, the initial injection time of AAV8-null/SYT7 or Trulicity was 4 months after $FeSO_4$ compound diet intake. In the rescue experiment of *db/db* mice, the initial injection time of AAV8-null/SYT7, Trulicity or Deferoxamine (DFO) was 3 weeks old.

Trulicity (1.5 mg/0.5 ml, Lilly) was injected subcutaneously into the groin with an injection dose of 1.08 mg/kg/week. The injection method of DFO (HY-B0988, MCE) in *db/db* mice was intraperitoneal injection with an injection dose of 50 mg/kg/day.

The INS level in the serum isolated from the whole blood collected after fasting (free drinking water) for 4 h in each group of mice was defined as the basal INS level.

### Intraductal pancreatic virus infusion

According to the method of Xiao et al. [15], AAV8-SYT7 or control virus (AAV8-null) (Vigene, Jinan, China) is diluted with PBS to $10^{12}$ genome copy particles (GCPs)/ml. AAV8-SYT7 or control virus is provided in the form of ssAAV, and the vector map was shown in Fig. S5A.

### Intraperitoneal glucose tolerance test (IPGTT) and intraperitoneal INS tolerance test (IPITT)

After fasting for 16 h, mice were injected with glucose (G8270, Sigma) (1.5 g/kg) IPGTT. For IPITT, INS (Novolin 50R, 300 IU/3 ml) was injected with 0.75 IU/kg on the mice after fasting for 4 h. At the set time point, we used the blood glucose meter (06870279001, Roche) to measure the blood glucose value of the tail vein, drawn the curve and calculated the area under the curve (AUC).

### Hyperglycemic clamps

According to the method of Zhu et al. [16], jugular vein implantation and hyperglycemic clamp experiments were conducted on each group of mice. The time of jugular vein implantation in mice of each group is shown in Supplementary Table 3. After fasting for 12 h, mice were subjected to hyperglycemic clamp test, and the glucose infusion rate was adjusted so that the blood glucose was clamped to 17 mM (± 1 mM) within 30 min after infusion. Blood samples were collected at the time point of 0, 5, 10, 20, and 30 min respectively after infusion. Then the INS content was detected by enzyme-linked immunosorbent assay (ELISA). 0–10 min was defined as the first stage of INS secretion, and 10–30 min was defined as the second stage of INS release.

### Cell culture and medication treatment

The mouse β cell line MIN6 was donated by Prof. Bin Xue (Shaw Hospital Affiliated to Nanjing Medical University). The Beta-TC-6 was purchased from National Collection

of Authenticated Cell Cultures. Both cell lines cultured in DMEM (glucose 1 g/L) containing 15% FBS, 1 mM sodium pyruvate and 50 μM β-mercaptoethanol (all from Gibco). Medium needs to be replaced every 24 h. The freshly prepared complete culture medium needs to be used up within a week. TH5487 (HY-125276, MCE) dissolved in DMSO was added to fresh MIN6 complete medium to a final concentration of 5 μM, and the control group was treated with the same amount of DMSO. The fresh culture medium was replaced every 24 h, and the supernatant and cells were collected after TH5487 treatment for 48 h.

The glucagon-like peptide-1 (GLP-1) was synthesized by Sangon Biotech (Shanghai, China). The sequence was HAEGTFTSDVSSYLEGQAAKEFIAWLVKGRG. Final concentration was 50 nM, and the fresh medium was replaced every 24 h. The supernatant and cells were collected 48 h after the treatment of GLP-1.

The $Fe^{2+}$-exposed cell model was established by culturing MIN6 cells in complete medium supplemented with 100 μM $FeSO_4$. Although $FeSO_4$ is considered not harmful and widely used as supplement to treat iron-deficiency anemia, however, drug dosage is an issue that must be considered, as high concentrations may be toxic to cells. Therefore, in our preliminary experiment, to avoid the toxicity of high dose of $FeSO_4$ to β cells, a normal human serum iron concentration of 20 μM was used as the initial reference value to evaluate the effect of different $FeSO_4$ concentrations on cell viability and INS release. The results showed that a $FeSO_4$ did not exert toxicity to β cells even with 3 mM $FeSO_4$ treatment, and a significant suppressive effect on INS release was observed in MIN6 cells starting at 100 μM $FeSO_4$. Therefore, 100 μM is a safe concentration of $FeSO_4$ for establishing the $Fe^{2+}$-exposed cell model. In this study, MIN6 cells were cultured with 100 μM $FeSO_4$-containing medium for 11 days with fresh medium replaced daily.

293T was purchased from National Collection of Authenticated Cell Cultures and cultured in DMEM (4.5 g/L glucose) containing 10% FBS. The medium was replaced every 48 h. The cell incubator was set to 37°C, 5% $CO_2$, and saturated humidity.

## Glucose-stimulated INS secretion (GSIS), potassium-stimulated INS secretion (KSIS) and INS content determination

The isolation and culture of islets were described in Zhu et al. [17]. The methods of GSIS/KSIS of MIN6 (or isolated islets) were as described in Huang et al. [18]. In the GSIS experiment, glucose was used at concentrations of 2.8 mM and 25 mM. In the KSIS experiment, potassium chloride was used at the concentration of 50 mM. The methods for determining INS secretion or content were carried out in accordance with the instructions of the ELISA (10-1249-01, Mercodia). INS secretion and INS content can be obtained after standardization with total protein.

## Electrophoretic mobility shift assay (EMSA)

EMSA was performed according to the method described previously [14], the probe (− 208 to − 156 bp) was designed according to the promoter region of *SYT7*. The final concentration of OGG1 (enz-253, PROSPEC) final concentration was 50 ng/μl in the reaction system. $Fe^{2+}$ was added in the form of an $FeSO_4{\cdot}7H_2O$ aqueous solution and dissolved before use (with final concentration 100 μM in reaction system).

## Western blot

Western blot experiments were carried out according to the method of Ci et al. [19]. The primary antibodies anti-OGG1 (sc-376835) and anti-synaptotagmin VII (sc-293343) were from Santa Cruz (diluted 1:200) and anti-INS (ab181547) was from Abcam (diluted 1:1000) and Anti-β-tubulin was from Abgent (AM1031A, diluted 1:1000).

## Statistical analysis

Quantitative data were obtained in triplicate from at least three independent experiments and are presented as the mean ± standard error and inferential statistics (*P* values). Statistical significance was evaluated using paired two-tailed Student's *t* tests. $P < 0.05$ was considered statistically significant. All statistical analyses were done using GraphPad Prism 8.0.

## Other assays

Cell transfection and dual luciferase reporter gene detection, intracellular $Ca^{2+}$ content detection, serum $Fe^{2+}$ content detection, hematoxylin and eosin (H&E) staining, immunofluorescence and oil red O staining, β cell mass, chromatin immunoprecipitation (ChIP)-qPCR, microarray analysis, transmission electron microscope (TEM) detection, cell viability assays, real-time quantitative PCR (RT-qPCR), retrospective analysis of patients with T2DM, more details about these assays are included in Supplementary Methods.

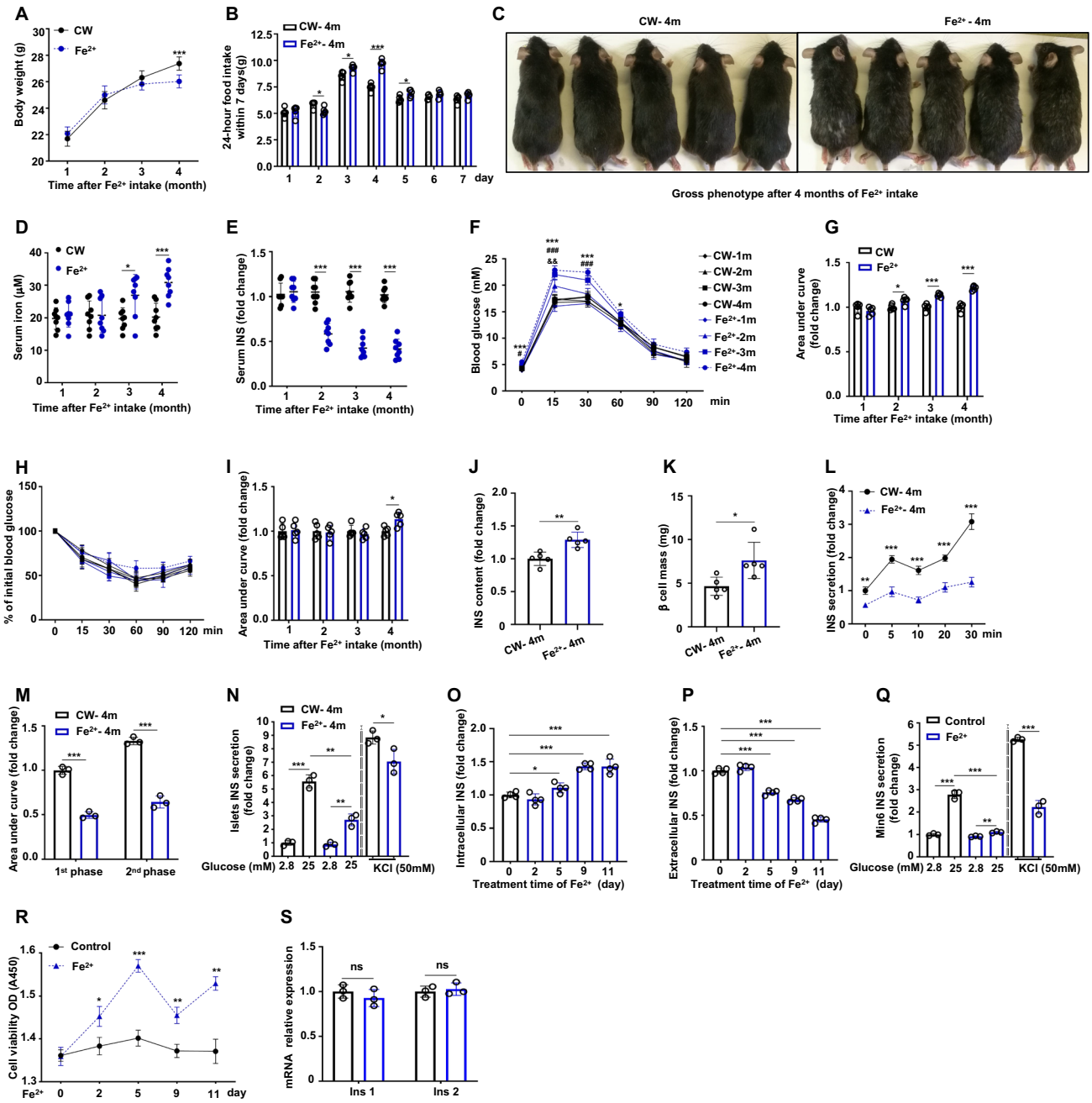


## Results

### Long-term high-dose $FeSO_4$ intake impairs INS secretion

Through analysis of mice with a long-term, high-dose $FeSO_4$ diet, it was found that the average weight was slightly lower than that of the CW mice when fed for 3 months, with significant weight loss at month 4 (Fig. 1A). However, food intake in the $Fe^{2+}$ mice group did not decrease (Fig. 1B). In terms of general appearance, the $Fe^{2+}$ mice had erect hair and lacked luster and became lighter in color (Fig. 1C). As expected, serum iron levels gradually increased with the duration of high-dose $FeSO_4$ intake (Fig. 1D), while serum INS levels gradually decreased (Fig. 1E).

We performed IPGTT and IPITT to evaluate the effect of high-dose $FeSO_4$ intake on glucose tolerance and INS tolerance. The data showed that in the $Fe^{2+}$ mice group, both the fasting blood glucose and blood glucose levels at 15, 30, and 60 min after glucose loading were significantly increased with the duration of $FeSO_4$ intake, and the AUC increased (Fig. 1F, G), while the glucose levels at all time point of IPITT were comparable to that of the CW group (Fig. 1H), and the AUC increased with $FeSO_4$ intake

◂**Fig. 1** Long-term high-dose $FeSO_4$ intake impairs INS secretion. **A** The weight changes of the mice after a high-dose $FeSO_4$ supplemented diet. $n=6$ in each cohort. $^{***}P<0.001$. **B** The amount of food consumed by the mice in $Fe^{2+}$ mice group per 24 h for one week after ingesting high-dose $FeSO_4$ for 4 months. $n=5$ in each cohort. $^{*}P<0.05$, $^{***}P<0.001$. **C** Gross phenotype of the $Fe^{2+}$ mice group fed a high-dose $FeSO_4$-supplemented diet for 4 months compared with the CW mice group. **D** Changes in serum iron content in the mice consuming high-dose $FeSO_4$-supplemented diets for 1–4 months. $n=8$ in each cohort. $^{*}P<0.05$, $^{***}P<0.001$. **E** Fold changes in serum INS content in the mice consuming high-dose $FeSO_4$-supplemented feed for 1–4 months compared to CW mice. $n=8$ in each cohort. $^{***}P<0.001$. **F**, **G** The results of the IPGTT experiment and the corresponding AUC of the mice in the CW mice group and the mice in the $Fe^{2+}$ mice group when they were fed a normal diet and high-dose $FeSO_4$ diet for 1–4 months. $n=5$ in each cohort. Mice were fed normal chow for 1 month, 2 months, 3 months and 4 months and are shown as cw-1m, cw-2m, cw-3m and cw-4m, respectively. Mice were fed high-dose $FeSO_4$-supplemented feed for 1 month, 2 months, 3 months and 4 months and are shown as $Fe^{2+}$-1m, $Fe^{2+}$-2m, $Fe^{2+}$-3m and $Fe^{2+}$-4m, respectively. *Indicates the $Fe^{2+}$-4m group compared with the CW-4m group, $^{*}P<0.05$, $^{***}P<0.001$. $^{\#}$: Indicates the $Fe^{2+}$-3m group compared with the CW-3m group, $^{\#}P<0.05$, $^{\#\#\#}P<0.001$. $^{\&}$Indicates the $Fe^{2+}$-2m group compared with the CW-2m group, $^{\&\&}P<0.01$. In the comparison of the AUC of each group, $^{*}P<0.05$, $^{***}P<0.001$. **H**, **I** The results of the IPITT experiment and corresponding AUC of the mice in the CW group and the mice in the $Fe^{2+}$ group when they were fed a normal diet and a high-dose $FeSO_4$ diet for 1–4 months. $n=5$ in each cohort. $^{*}P<0.05$. **J** ELISA show that fold changes in INS content in isolated islets of $Fe^{2+}$-4m and CW-4m mice. $n=5$ in each cohort. $^{**}P<0.01$. **K** β cell mass of isolated islets of mice in $Fe^{2+}$-4m group. $n=5$ in each cohort. $^{*}P<0.05$. **L**, **M** Hyperglycemic clamp tests show INS biphasic secretion and AUC when high-dose $FeSO_4$ diet for 4 months. 0–10 min is defined as the first phase and 10–30 min is defined as the second phase. $n=3$ in each cohort. $^{**}P<0.01$, $^{***}P<0.001$. **N** GSIS/KSIS levels in isolated islets of mice in $Fe^{2+}$-4m group. **O** ELISA results showed fold changes in intracellular INS content in MIN6 cells after $FeSO_4$ (100 μM) treatment for 2–11 days compared to 0 day. **P** Fold changes in INS level in the supernatant of MIN6 culture medium after treatment with $FeSO_4$ (100 μM) for 2–11 days compared to 0 day. **Q** GSIS and KSIS levels in the MIN6 cells exposed to $Fe^{2+}$ for 11 days. **R** The viability of the MIN6 cells treated with $FeSO_4$ for 0–11 days. **S** The expression level of *Ins1/Ins2* mRNA in MIN6 cells treated with $FeSO_4$ for 11 days. **N**–**S**, data are presented as mean ± s.d. of at least three separate experiments. $^{*}P<0.05$, $^{**}P<0.01$, $^{***}P<0.001$, *ns* no significant difference

for 4 months (Fig. 1I). Although INS content of islets (Fig. 1J) and β cell mass (Fig. 1K) were increased after high dose iron intake, the results of hyperglycemia clamp tests (Fig. 1L, M) and INS release tests of isolated islets (Fig. 1N) showed that long term high dose iron intake decreased the INS secretion level. To determine whether $Fe^{2+}$ exposure directly impairs β cell function, we cultured the mouse β cell line MIN6 in complete medium containing 100 μM $FeSO_4$. The intracellular INS content showed an upward trend with prolonged incubation time (Fig. 1O). However, after 5 days of incubation, the INS content in the supernatant of MIN6 culture medium with $FeSO_4$ was significantly reduced, and to approximately 50% of that of the control group after 11 days (Fig. 1P). The INS secretion response to glucose and potassium chloride stimulation decreased (Fig. 1Q). Corresponding to the reduced level of INS secretion, the intracellular $Ca^{2+}$ content was also reduced (Fig. S1A, B). Furthermore, cell vitality assays showed that 100 μM $FeSO_4$ treatment slightly increased cell viability (Fig. 1R), which excluded the effects of cell growth. Such increase may be due to an adaptation of β cells to the environmental stress and compensation for the damaged secretion function. RT-qPCR results showed that this effect was not caused by INS transcription (Fig. 1S). Overall, these results suggest that high doses of $FeSO_4$ significantly inhibited the INS secretion of β cells before compromising cell viability.

## OGG1 deficiency impaired INS secretion

Recent studies have suggested that oxidative stress is the main cause of islet β cell dysfunction induced by excessive iron [20]. Since OGG1 is constitutively expressed as a housekeeping enzyme in response to oxidative stress in living cells, OGG1 deficiency is closely related to metabolic disorders [21]. We then suspected that OGG1 may be the candidate molecule involved in excessive iron-inhibited INS secretion. To test this hypothesis, we examined the phenotype in WT ($Ogg1^{+/+}$) and *Ogg1* knockout ($Ogg1^{-/-}$) mice (Fig. S2A, B). The body weight of mice was slightly decreased with *Ogg1* knockout and this was not due to the reduced food intake (Fig. 2A, Fig. S2C). Notably, random blood glucose was slightly elevated (Fig. 2B), while serum INS levels were significantly reduced in the $Ogg1^{-/-}$ mice (Fig. 2C). The IPGTT results showed that blood glucose of $Ogg1^{-/-}$ mice increased significantly at 15 min and 30 min after glucose loading (Fig. 2D), and the AUC increased (Fig. 2E). IPITT data showed no significant difference between the two groups (Fig. 2F, G). $Ogg1^{-/-}$ mice exhibited increased intracellular INS level in β cells (Fig. 2H, I). The hyperglycemic clamp experiment demonstrated an attenuated INS secretion level in $Ogg1^{-/-}$ mice (Fig. 2J, K). Moreover, isolated islets from the $Ogg1^{-/-}$ mice showed impaired GSIS (Fig. 2L) and decreased intracellular $Ca^{2+}$ content (Fig. S3A). Next, similar results were obtained in MIN6 cells with *Ogg1* knockdown by shRNA (Fig. 2M–R, Fig. S3B, C) or with the OGG1 inhibitor TH5487 treatment (Fig. 2R–V, Fig. S3D, E). Thus, the data suggest that OGG1 plays an important role in glucose-stimulated INS secretion.

## *SYT7* is a new downstream target gene of OGG1

As OGG1 is involved in the regulation of gene expression [11–14], searching the appropriate downstream target gene may be the effective way to investigate OGG1 physiological function. We compared the gene expression of $Ogg1^{+/+}$ and $Ogg1^{-/-}$ mouse embryonic fibroblasts (MEFs) by microarray

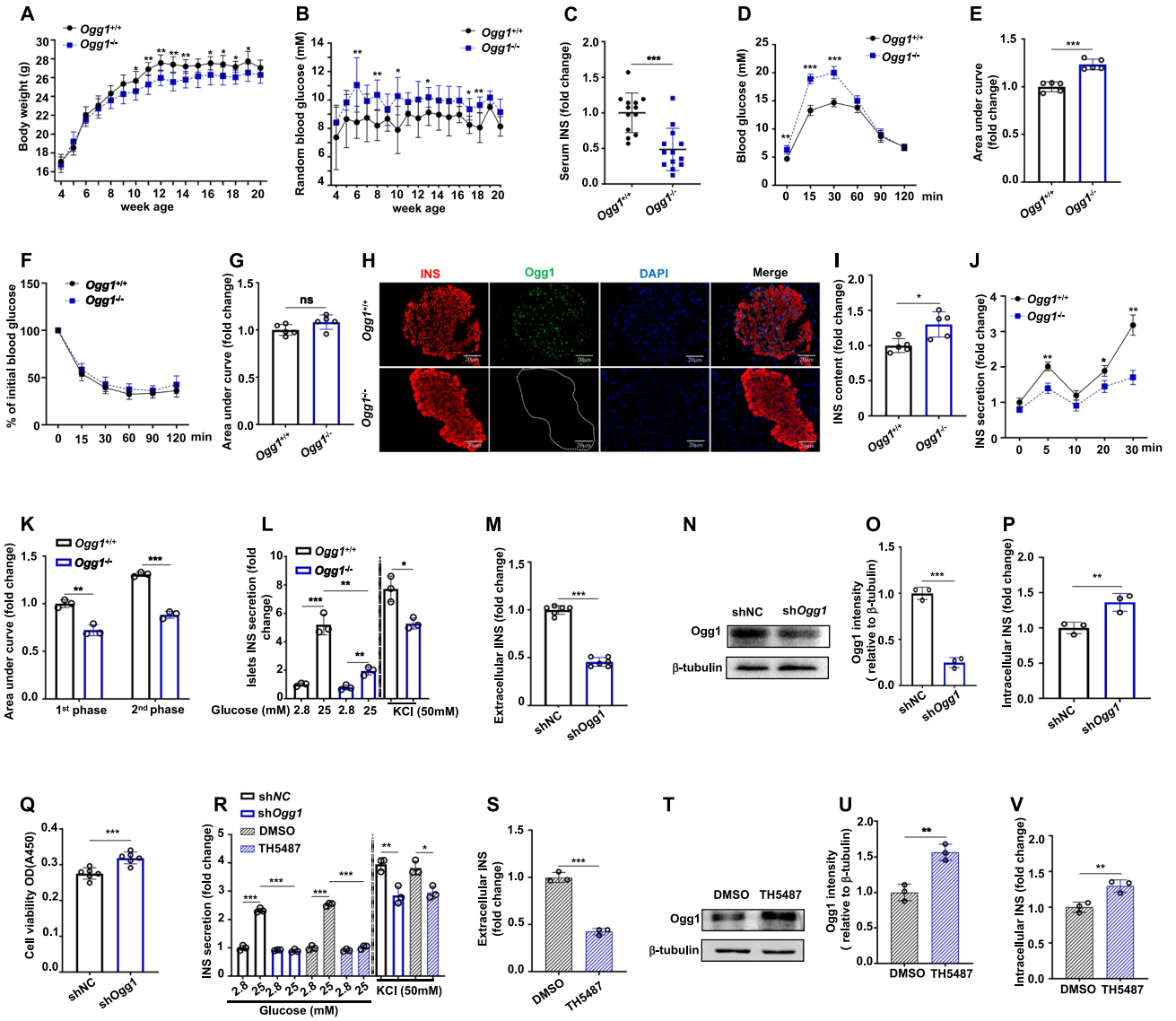


**Fig. 2** OGG1 deficiency impaired INS secretion. **A** Weight changes of the $Ogg1^{-/-}$ and $Ogg1^{+/+}$ mice aged 4–20 weeks. $n=6$ in each cohort. $^{*}P<0.05$, $^{**}P<0.01$. **B** Random blood glucose of the $Ogg1^{-/-}$ and $Ogg1^{+/+}$ mice aged 4–20 weeks. $n=6$ in each cohort. $^{*}P<0.05$, $^{**}P<0.01$. **C** Serum INS content in the $Ogg1^{-/-}$ and $Ogg1^{+/+}$ mice aged 6 weeks, $n=13$ in each cohort. $^{***}P<0.001$. **D**, **E** The results of the $Ogg1^{-/-}$ and $Ogg1^{+/+}$ mice aged 6 weeks detected by IPGTT and the corresponding AUC. $n=5$ in each cohort. $^{**}P<0.01$, $^{***}P<0.001$. **F**, **G** The results of the $Ogg1^{-/-}$ and $Ogg1^{+/+}$ mice aged 6 weeks detected by IPITT and the corresponding AUC. $n=5$ in each cohort. ns, no significant difference. **H**, **I** **H** The levels of Ogg1 in islets of the $Ogg1^{-/-}$ and $Ogg1^{+/+}$ mice aged 6 weeks were detected by immunofluorescence. **I** The levels of INS in islets of the $Ogg1^{-/-}$ and $Ogg1^{+/+}$ mice aged 6 weeks were detected by ELISA. $n=5$ in each cohort. $^{*}P<0.05$. Scale bar 20 μm. **J**, **K** Hyperglycemic clamp tests show INS biphasic secretion and AUC in $Ogg1^{-/-}$ and $Ogg1^{+/+}$ mice aged 6 weeks. 0–10 min is defined as the first phase and 10–30 min is defined as the second phase. $n=3$ in each cohort. $^{*}P<0.05$, $^{**}P<0.01$, $^{***}P<0.001$. **L** GSIS and KSIS levels in islets of the $Ogg1^{-/-}$ and $Ogg1^{+/+}$ mice aged 6 weeks. Data are presented as mean ± s.d. of three separate experiments. $^{*}P<0.05$, $^{**}P<0.01$, $^{***}P<0.001$. **M** The INS level in the supernatant of MIN6 cells after knockdown of *Ogg1* were detected by ELISA. Data are presented as mean ± s.d. of six separate experiments. $^{***}P<0.001$. **N**–**P** **N** *Ogg1* knockdown in MIN6 cell line and Ogg1 content. O, the gray analysis statistical value of three independent experiments. **P** detection of intracellular INS level after shOgg1 by ELISA. **Q** Cell viability of MIN6 cells with *Ogg1* knockdown was detected by CCK8 assay. **R** The effect of knocking down *Ogg1* and using OGG1 inhibitor TH5487 on GSIS and KSIS levels in MIN6 cells. **S** The INS secretion level of MIN6 with OGG1 inhibitor TH5487 treatment were detected by ELISA. **T**–**V** **T** The Ogg1 content of MIN6 cells with or without Th5487 treatment. **U** The gray analysis statistical value of three independent experiments. **V** ELISA results show the fold changes in intracellular INS levels after Th5487 pretreatment compared to DMSO. **N**–**V** Data are presented as mean ± s.d. of three separate experiments. $^{*}P<0.05$, $^{**}P<0.01$, $^{***}P<0.001$

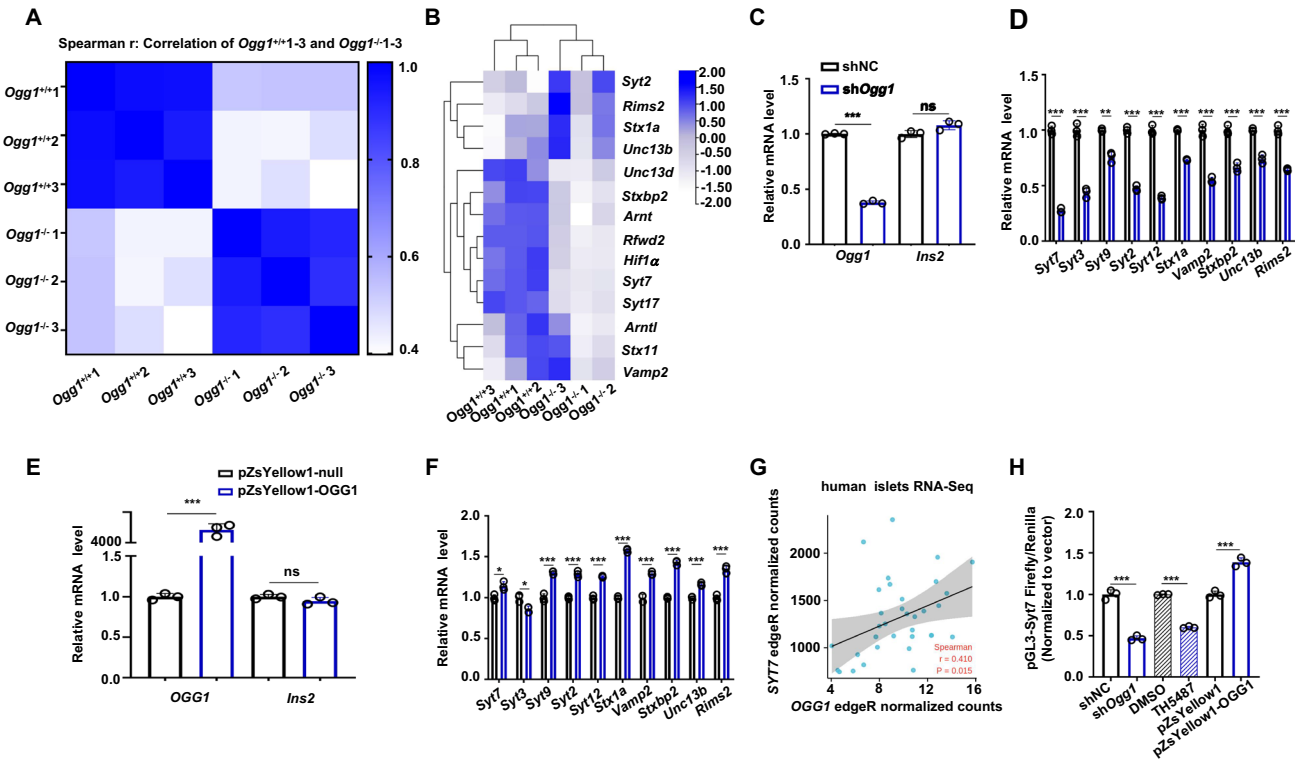


**Fig. 3** *SYT7* is a new downstream target gene of OGG1. **A**, **B** The $Ogg1^{+/+}$ and $Ogg1^{-/-}$ MEF gene microarray test results. $n=3$ in each cohort. **C**, **D** Gene expression in MIN6 cells after knockdown of *Ogg1*. Data are presented as mean ± s.d. of three separate experiments. $^{**}P<0.01$, $^{***}P<0.001$. *ns* no significant difference. **E**, **F** Gene expression in MIN6 cells after overexpression of *OGG1*. Data are presented as mean ± s.d. of three separate experiments. $^{*}P<0.05$, $^{***}P<0.001$, *ns* no significant difference. **G** RNA-Seq data in the GEO database show the correlation between *OGG1* and *SYT7* expression in human β cells (data from GEO: GSE165121). Spearman related analysis. $P=0.015$. **H** Double luciferase reporter system was used to detect the effect of *Ogg1* knockdown, TH5497 and *OGG1* overexpression on the fluorescence signal intensity of pGL3-Syt7. Data are presented as mean ± s.d. of three separate experiments. $^{***}P<0.001$

from our previous study. The results showed that 14 of the genes affected by *Ogg1* knockout involved in the INS secretion process [22–29], of which 10 genes were significantly downregulated (Fig. 3A, B). Since MEFs are characterized by their ability to secrete cytokines [30], such downregulation may also be present in INS-secreting cells. To confirm the microarray results in β cells, we performed RT-qPCR in MIN6 cells with *Ogg1* knockdown or overexpression. The results show that there was no significant difference in the expression level of the *Ins2* gene (Fig. 3C, E); however, the expression of 10 genes, such as *Syt7*, was significantly changed (Fig. 3D, F). SYTs family members play crucial roles in the regulatory exocytosis of the nervous and endocrine systems [31]. To investigate whether there is a relationship between *OGG1* and *SYT7*, we used public RNA-seq data from the Gene Expression Omnibus (GEO) and analyzed the expression of *OGG1* and *SYT7* in islets from healthy people (GEO: GSE165121). The data showed a positive correlation between the two genes (Fig. 3G). It has been established that under oxidative stress, one important role of OGG1 is binding to oxidized guanine and participating in gene transcriptional regulation [32]. To explore whether OGG1 is involved in *SYT7* transcription, we performed a classic dual-luciferase reporter assay. The results show that both *Ogg1* knockdown and inhibitor treatment noticeably decreased the luciferin signal, while *OGG1* overexpression increased the signal, which suggested that *SYT7* is a new transcriptional target of OGG1 (Fig. 3H).

## OGG1/SYT7 is indispensable for INS secretion

To determine whether SYT7 is the exact downstream protein mediating OGG1 effect on INS secretion, we overexpressed SYT7 in *Ogg1*-knockdown MIN6 cells. SYT7 overexpression significantly reversed the increase of intracellular INS levels and the decrease of extracellular INS levels induced by Ogg1 deficiency (Fig. 4A–D). Correspondingly, the reduced intracellular $Ca^{2+}$ content also partially rescued (Fig. S4A). To explore the important role of OGG1/SYT7 in INS secretion, we first chose GLP-1 (an incretin hormone increasing

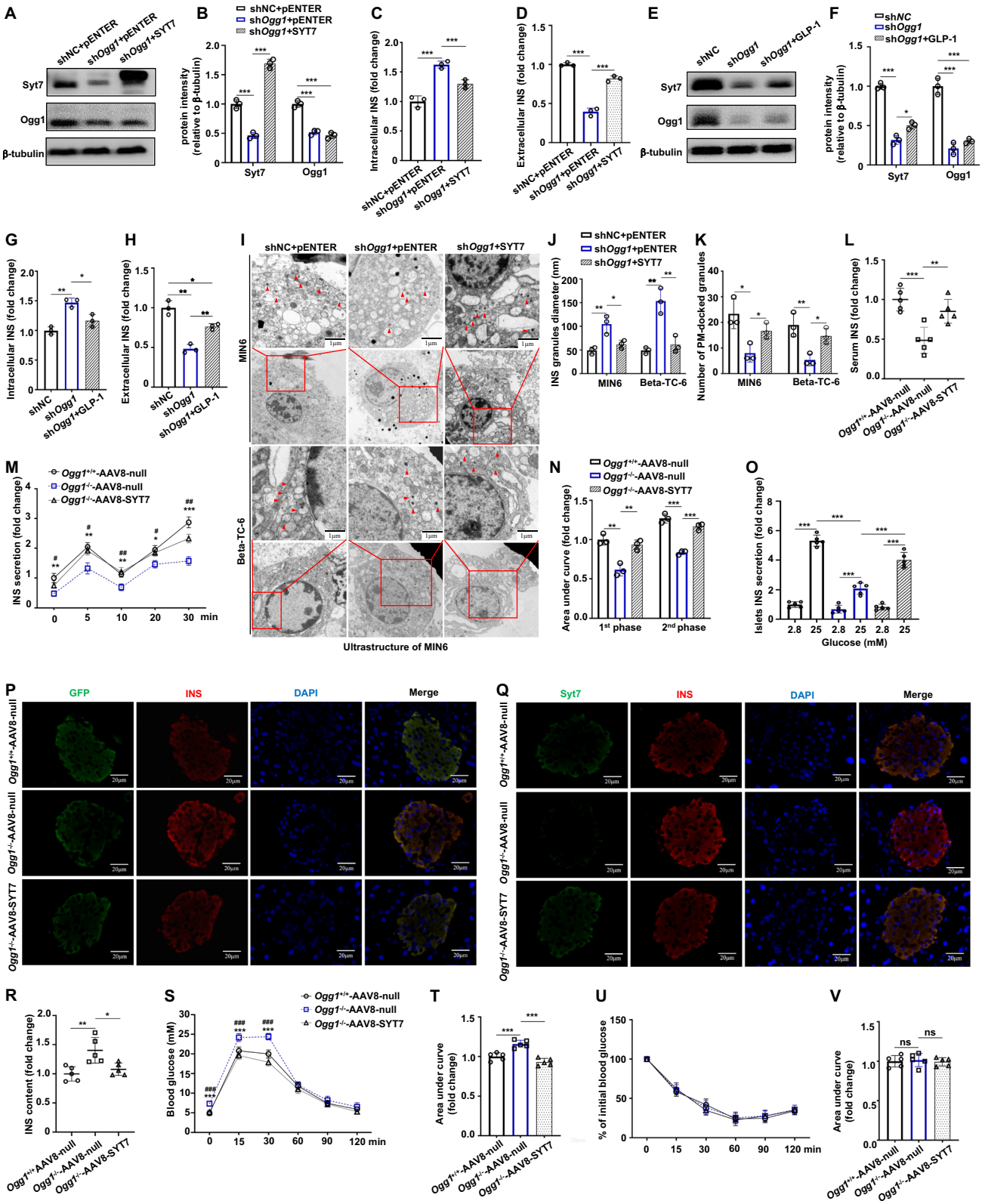
A
shNC+pENTER
shOgg1+pENTER
shOgg1+SYT7
Syt7
Ogg1
β-tubulin
B
shNC+pENTER
shOgg1+pENTER
shOgg1+SYT7
protein intensity (relative to β-tubulin)
Syt7
Ogg1
C
Intracellular INS (fold change)
D
Extracellular INS (fold change)
E
shNC
shOgg1
shOgg1+GLP-1
Syt7
Ogg1
β-tubulin
F
shNC
shOgg1
shOgg1+GLP-1
protein intensity (relative to β-tubulin)
Syt7
Ogg1
G
Intracellular INS (fold change)
shNC
shOgg1
shOgg1+GLP-1
H
Extracellular INS (fold change)
shNC
shOgg1
shOgg1+GLP-1
I
shNC+pENTER
shOgg1+pENTER
shOgg1+SYT7
MIN6
Beta-TC-6
Ultrastructure of MIN6
J
shNC+pENTER
shOgg1+pENTER
shOgg1+SYT7
INS granules diameter (nm)
MIN6
Beta-TC-6
K
Number of PM-docked granules
MIN6
Beta-TC-6
L
Serum INS (fold change)
Ogg1+/+-AAV8-null
Ogg1-/--AAV8-null
Ogg1-/--AAV8-SYT7
M
Ogg1+/+-AAV8-null
Ogg1-/--AAV8-null
Ogg1-/--AAV8-SYT7
INS secretion (fold change)
min
N
Ogg1+/+-AAV8-null
Ogg1-/--AAV8-null
Ogg1-/--AAV8-SYT7
Area under curve (fold change)
1st phase
2nd phase
O
Islets INS secretion (fold change)
Glucose (mM)
P
GFP
INS
DAPI
Merge
Ogg1+/+-AAV8-null
Ogg1-/--AAV8-null
Ogg1-/--AAV8-SYT7
Q
Syt7
INS
DAPI
Merge
Ogg1+/+-AAV8-null
Ogg1-/--AAV8-null
Ogg1-/--AAV8-SYT7
R
INS content (fold change)
Ogg1+/+-AAV8-null
Ogg1-/--AAV8-null
Ogg1-/--AAV8-SYT7
S
Ogg1+/+-AAV8-null
Ogg1-/--AAV8-null
Ogg1-/--AAV8-SYT7
Blood glucose (mM)
min
T
Area under curve (fold change)
Ogg1+/+-AAV8-null
Ogg1-/--AAV8-null
Ogg1-/--AAV8-SYT7
U
% of initial blood glucose
min
V
ns
Area under curve (fold change)
Ogg1+/+-AAV8-null
Ogg1-/--AAV8-null
Ogg1-/--AAV8-SYT7

◂**Fig. 4** OGG1/SYT7 is indispensable for INS secretion. **A**–**C** **A** The SYT7 level in *Ogg1*-knockdown MIN6 cells with *SYT7* overexpression. **B** The gray analysis statistical value of three independent experiments. **C** Intracellular INS level in *Ogg1*-knockdown MIN6 cells with *SYT7* overexpression. Data are presented as mean ± s.d. of three separate experiments. ***$P<0.001$. **D** The content of INS in cell culture supernatant from *Ogg1*-knockdown MIN6 cells with SYT7 overexpression. Data are presented as mean ± s.d. of three separate experiments. ***$P<0.001$. **E**–**G** **E** Syt7 level of *Ogg1*-knockdown MIN6 cells treated with GLP-1 were detected by Western blot. **F** The gray analysis statistical value of three independent experiments. **G** Intracellular INS level of *Ogg1*-knockdown MIN6 cells treated with GLP-1 were detected by ELISA. Data are presented as mean ± s.d. of three separate experiments. *$P<0.05$, **$P<0.01$, ***$P<0.001$. **H** The INS level in the supernatant of the cell culture medium of *Ogg1*-knockdown MIN6 cells treated with GLP-1 was detected by ELISA. Data are presented as mean ± s.d. of three separate experiments. *$P<0.05$, **$P<0.01$. **I**–**K** **I** The intracellular ultrastructure of MIN6 and Beta-TC-6 cells. Scale bar 1 μm. **J** The average INS granules diameter in cells of each group. **K** Number of PM docked granules in each group. Data are presented as mean ± s.d. of three separate experiments. *$P<0.05$, **$P<0.01$. **L** Serum basal INS levels in $Ogg1^{-/-}$ mice 3 weeks after AAV8-SYT7 injection. $n=5$ in each cohort. **$P<0.01$, ***$P<0.001$. **M**, **N** Hyperglycemic clamp tests show INS biphasic secretion and AUC in $Ogg1^{-/-}$ mice 3 weeks after AAV8-SYT7 injection. 0–10 min is defined as the first phase and 10–30 min is defined as the second phase. $n=3$ in each cohort. *Indicates the $Ogg1^{-/-}$-AAV8-null group compared with the $Ogg1^{+/+}$-AAV8-null group, *$P<0.05$, **$P<0.01$, ***$P<0.001$. $^{\#}$Indicates the $Ogg1^{-/-}$-AAV8-SYT7 group compared with the $Ogg1^{-/-}$-AAV8-null group, $^{\#}P<0.05$, $^{\#\#}P<0.01$. In the comparison of the AUC of each group, **$P<0.01$, ***$P<0.001$. **O** GSIS levels of isolated islets from $Ogg1^{-/-}$ mice 3 weeks after AAV8-SYT7 injection. $n=5$ in each cohort. **$P<0.01$, ***$P<0.001$. **P**, **Q** The expression of the AAV8 vector tag GFP and Syt7 in the islets of the $Ogg1^{+/+}$-AAV8-null, $Ogg1^{-/-}$-AAV8-null and $Ogg1^{-/-}$-AAV8-SYT7 mice 3 weeks after AAV8-SYT7 injection were detected by immunofluorescence. Scale bar 20 μm. **R** INS content in isolated islets from $Ogg1^{-/-}$ mice 3 weeks after AAV8-SYT7 injection. $n=5$ in each cohort. *$P<0.05$, **$P<0.01$. **S**, **T** $Ogg1^{-/-}$-AAV8-SYT7 mice 3 weeks after AAV8-SYT7 injection, the results of the IPGTT experiment and the corresponding AUC. $n=5$ in each cohort. For **S**, *Indicates the $Ogg1^{-/-}$-AAV8-null group compared with the $Ogg1^{+/+}$-AAV8-null group, ***$P<0.001$. $^{\#}$Indicates the $Ogg1^{-/-}$-AAV8-SYT7 group compared with the $Ogg1^{-/-}$-AAV8-null group, $^{\#\#\#}P<0.001$. In the comparison of the AUC of each group, ***$P<0.001$. **U**, **V** $Ogg1^{-/-}$-AAV8-SYT7 mice 3 weeks after AAV8-SYT7 injection, the results of the IPITT experiment and the corresponding AUC. $n=5$ in each cohort. ns, no significant difference

INS secretion in glucose-dependent manner) to evaluate whether OGG1 deficiency-induced INS secretion dysfunction could be rescued by this peptide. Results showed that although the extracellular INS level and $Ca^{2+}$ content in the *Ogg1*-knockdown group were significantly increased by GLP-1, it was still lower than those in the control group (Fig. 4E, H, Fig. S4B), which suggests that OGG1/SYT7 was very important for INS secretion. The TEM images showed that *Ogg1* knockdown increased the volume of INS granules and reduced the number of INS granules docked on the plasma membrane (PM). Importantly, these phenotypes were restored after SYT7 overexpression (Fig. 4I–K). Next, we injected AAV8-SYT7 into the $Ogg1^{-/-}$ mice in situ through the bile duct to examine the recovery effect of SYT7. Our data showed that serum INS level, INS biphasic secretion and extracorporeal GSIS of islets were increased (Fig. 4L–O), and no damage to major organs was detected with AAV8-SYT7 injection (Fig. S5B). The immunofluorescence and ELISA results show that the intracellular INS level was decreased with the successful expression of SYT7 in islets (Fig. 4P–R). IPGTT results demonstrated that AAV8-SYT7 injection significantly decreased the blood glucose level of $Ogg1^{-/-}$ mice (Fig. 4S, T). No significant change was observed by IPITT (Fig. 4U, V). Taken together, the data suggest that OGG1/SYT7 is indispensable for INS secretion.

## Excessive iron inhibited OGG1 binding to the *SYT7* promoter

Our data have shown that high-does iron increased Ogg1 protein levels in islets. However, contrary to expectation, Syt7 expression was gradually decreased (Fig. 5A, B), which is contradictory to the positive correlation between the two genes. Since OGG1 binding to the substrate could be inhibited by heavy metal [33], we then speculate whether excessive iron has the similar effect. To test this hypothesis, we first detected the expression level of *Syt7* in MIN6 cells cultured with 100 μm $FeSO_4$ in different time periods. The RT-qPCR results showed that the mRNA level of *Syt7* gradually decreased with culture time and was approximately 0.6-fold of the untreated group on the 11th day (Fig. 5C). Interestingly, by screening the RNA-seq data of the GEO database (GSE128945), we also found that *Ogg1* expression was upregulated and *Syt7* expression was downregulated in β cells of β-DKO mice whose islet function was destroyed (conditional knockout of *Swi/Snf* genes, which encode SWI/SNF chromatin-remodeling complex controlling the induction of iron transport genes), showing a negative correlation (Fig. 5D, E). To verify whether $FeSO_4$ directly impairs the binding of OGG1 to the *SYT7* promoter, we synthesized the *SYT7* promoter sequence and carried out an EMSA with purified recombinant OGG1 protein. The results showed that OGG1 specifically bound with 8-oxoG and the binding was abolished by $FeSO_4$ (Fig. 5F). ChIP-qPCR result was consistent with that of EMSA (Fig. 5G). Notably, the dual luciferase reporter assay showed that even in the case of overexpression of OGG1, the luciferin signal was still strongly suppressed by $FeSO_4$, which stressed the inhibitory effect of iron on the transcriptional regulatory function of OGG1 (Fig. 5H). These results also suggest that SYT7 may be an effector of $FeSO_4$ and OGG1 deficiency, leading to insufficient INS secretion. Next, to determine whether SYT7 can improve the impaired INS secretion caused by long-term high-dose $FeSO_4$ intake. We performed IPGTT and IPITT assay in iron overload mice with AAV-SYT7 injection. At

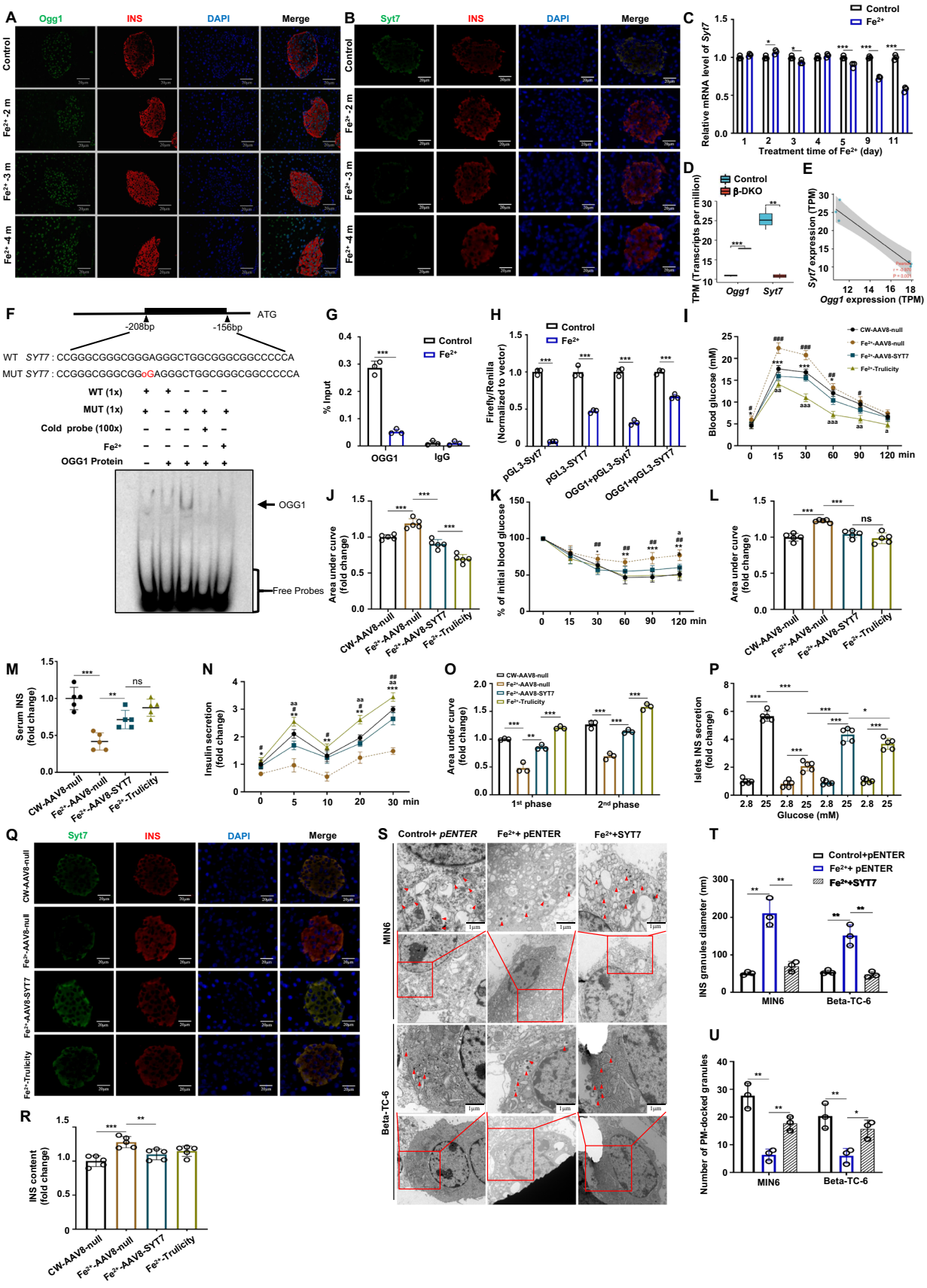
A
Ogg1
INS
DAPI
Merge
Control
Fe2+ -2 m
Fe2+ -3 m
Fe2+ -4 m
B
Syt7
INS
DAPI
Merge
C
Control
Fe2+
Relative mRNA level of Syt7
Treatment time of Fe2+ (day)
D
Control
β-DKO
TPM (Transcripts per million)
Ogg1
Syt7
E
Syt7 expression (TPM)
Ogg1 expression (TPM)
F
ATG
-208bp
-156bp
WT SYT7 : CCGGGCGGGCGGGAGGGCTGGCGGGCGGCCCCCA
MUT SYT7 : CCGGGCGGGCGGoGAGGGCTGGCGGGCGGCCCCCA
WT (1x)
MUT (1x)
Cold probe (100x)
Fe2+
OGG1 Protein
OGG1
Free Probes
G
Control
Fe2+
% Input
OGG1
IgG
H
Control
Fe2+
Firefly/Renilla (Normalized to vector)
pGL3-Syt7
pGL3-SYT7
OGG1+pGL3-Syt7
OGG1+pGL3-SYT7
I
CW-AAV8-null
Fe2+-AAV8-null
Fe2+-AAV8-SYT7
Fe2+-Trulicity
Blood glucose (mM)
min
J
Area under curve (fold change)
CW-AAV8-null
Fe2+-AAV8-null
Fe2+-AAV8-SYT7
Fe2+-Trulicity
K
% of initial blood glucose
min
L
Area under curve (fold change)
ns
M
Serum INS (fold change)
ns
N
Insulin secretion (fold change)
min
O
Area under curve (fold change)
1st phase
2nd phase
P
Islets INS secretion (fold change)
Glucose (mM)
Q
Syt7
INS
DAPI
Merge
CW-AAV8-null
Fe2+-AAV8-null
Fe2+-AAV8-SYT7
Fe2+-Trulicity
R
INS content (fold change)
S
Control+ pENTER
Fe2+ pENTER
Fe2+SYT7
MIN6
Beta-TC-6
T
Control+pENTER
Fe2+ pENTER
Fe2+SYT7
INS granules diameter (nm)
MIN6
Beta-TC-6
U
Number of PM-docked granules
MIN6
Beta-TC-6

◂**Fig. 5** Excessive iron inhibited OGG1 binding to the *SYT7* promoter. **A**, **B** Immunofluorescence staining of Ogg1, INS and Syt7 proteins in mouse β cells with $FeSO_4$ intake for 2–4 months. Scale bar 20 μm. **C** The relative expression of the *Syt7* gene in the MIN6 cells treated with $FeSO_4$ for 1, 2, 3, 4, 5, 9, and 11 days. Data are presented as mean ± s.d. of three separate experiments. $^*P<0.05$, $^{***}P<0.001$. **D**, **E** The expression of *Ogg1* and *Syt7* in mouse β cells were detected by RNA-seq. (data from GEO: GSE128945). $n=3$ in each cohort. $^{**}P<0.01$, $^{***}P<0.001$. **E** Person related analysis. $P=0.001$. **F** EMSA shows the binding of OGG1 to the *SYT7* promoter after $FeSO_4$ (100 μM) treatment. **G** ChIP-qPCR analysis of Ogg1 binding to the *Syt7* promoter in MIN6 cells treated with $FeSO_4$. Data are presented as mean ± s.d. of three separate experiments. $^{***}P<0.001$. **H** Dual luciferase reporter analysis of the effect of $FeSO_4$ treatment on *Syt7* promoter activity in 293 T cells with OGG1 overexpression. Firefly luciferase activity was measured 24 h post transfection and normalized to Renilla luciferase activity. Data are presented as mean ± s.d. of three separate experiments. $^{***}P<0.001$. **I**, **J** $Fe^{2+}$-4m mice 3 weeks after AAV8-SYT7 or Trulicity injection, the results of the IPGTT experiment and the corresponding AUC. $n=5$ in each cohort. *Indicates the $Fe^{2+}$-AAV8-null group compared with the CW-AAV8-null group, $^*P<0.05$, $^{***}P<0.001$. $^{\#}$Indicates that the $Fe^{2+}$-AAV8-SYT7 group was compared with the $Fe^{2+}$-AAV8-null group. $^{\#}P<0.05$, $^{\#\#}P<0.01$, $^{\#\#\#}P<0.001$. $^{a}$Indicates that the $Fe^{2+}$-Trulicity group was compared with the $Fe^{2+}$-AAV8-SYT7 group, $^{a}P<0.05$, $^{aa}P<0.01$, $^{aaa}P<0.001$. In the comparison of the AUC of each group, $^{***}P<0.001$. **K**, **L** $Fe^{2+}$-4m mice 3 weeks after AAV8-SYT7 or Trulicity injection, the results of IPITT experiment and corresponding AUC. $n=5$ in each cohort. *Indicates the $Fe^{2+}$-AAV8-null group compared with the CW-AAV8-null group, $^*P<0.05$, $^{**}P<0.01$, $^{***}P<0.001$. $^{\#}$Indicates that the $Fe^{2+}$-AAV8-SYT7 group was compared with the $Fe^{2+}$-AAV8-null group. $^{\#\#}P<0.01$. $^{a}$Indicates that the $Fe^{2+}$-Trulicity group was compared with the $Fe^{2+}$-AAV8-SYT7 group, $^{a}P<0.05$. In the comparison of the AUC of each group, $^{***}P<0.001$, *ns* no significant difference. **M** Serum basal INS content of $Fe^{2+}$-4m mice 3 weeks after AAV8-SYT7 or Trulicity injection. $n=5$ in each cohort. $^{**}P<0.01$, $^{***}P<0.001$. ns, no significant difference. **N**, **O** Hyperglycemic clamp tests show INS biphasic secretion and AUC of $Fe^{2+}$-4m mice 3 weeks after AAV8-SYT7 or Trulicity injection. 0–10 min is defined as the first phase and 10–30 min is defined as the second phase. $n=3$ in each cohort. **N** *Indicates the $Fe^{2+}$-AAV8-null group compared with the CW-AAV8-null group, $^*P<0.05$, $^{**}P<0.01$, $^{***}P<0.001$. $^{\#}$Indicates the $Fe^{2+}$-AAV8-SYT7 group compared with the $Fe^{2+}$-AAV8-null group, $^{\#}P<0.05$, $^{\#\#}P<0.01$. $^{a}$Indicates that the $Fe^{2+}$-Trulicity group was compared with the $Fe^{2+}$-AAV8-SYT7 group, $^{aa}P<0.01$. In the comparison of the AUC of each group, $^{**}P<0.01$, $^{***}P<0.001$. **P** Effect of AAV8-SYT7 injection on GSIS of isolated islets in each group. $n=5$ in each cohort. $^*P<0.05$, $^{***}P<0.001$. **Q** After 3 weeks of $Fe^{2+}$-4m mice 3 weeks injected with AAV8-SYT7 or Trulicity, immunofluorescence show the staining of Syt7 in the β cells of each group. Scale bar 20 μm. **R** The effect of AAV8-SYT7 on the INS content in islets in each group was detected by ELISA. $n=5$ in each cohort. $^{**}P<0.01$, $^{***}P<0.001$. **S**–**U** **S** The intracellular ultrastructure of MIN6 and Beta-TC-6 $Fe^{2+}$ model after SYT7 overexpression. Scale bar 1 μm. **T** The average INS granules diameter in cells of each group. **U** Number of PM docked granules in each group. Data are presented as mean ± s.d. of three separate experiments. $^*P<0.05$, $^{**}P<0.01$

the same time, Trulicity, a long-acting GLP-1 RA preparation promoting INS secretion, was also used as a positive control. The result showed that AAV8-SYT7 injection reversed the effect of $FeSO_4$ and improved glucose tolerance and INS sensitivity (Fig. 5I–L). The decreased serum INS level, the impaired biphasic INS secretion and GSIS levels of isolated islets induced by high-does iron feeding were all restored by AAV8-SYT7 (Fig. 5M–P). Immunofluorescence and isolated islets ELISA results further confirmed that AAV8-SYT7 decreased the INS content accumulated in β cells (Fig. 5Q, R). In addition, the ultrastructure showed that SYT7 overexpression partially restored the volume of INS granules and the number of INS granules docked on PM (Fig. 5S–U). In conclusion, these results suggest that iron exposure inhibits the binding of OGG1 to the *SYT7* promoter and suppresses *SYT7* transcription. Overexpression of SYT7 can improve the decrease in INS secretion levels, the reduction in secretory vesicles numbers and the increase in blood glucose levels caused by iron overload.

## Overexpression of SYT7 restored the impaired INS secretion in *db/db* mice

Islet β cell dysfunction is the key determinant of T2DM [34]. At present, the treatment of T2DM is mainly focused on oral hypoglycemic drugs and INS injections. However, what cannot be avoided is that β cell dysfunction continues to deteriorate with the passage of time [35]. Our retrospective analysis of 130 T2DM cases showed the ability of endogenous INS in response to the glucose load of β cells gradually decreased with the extension of medical history (Fig. S6), which is consistent with the discovery of Fonseca et al. [35]. Because *db/db* mice are animal models of INS resistance similar to human T2DM, and they also exhibit iron overload [36], we then used these mice to continuously detect the serum basal INS level from 3 weeks of age. The results show that *db/db* mice aged 3–6 weeks exhibited lower serum INS level than the WT group (Fig. 6A), indicating that iron overload-induced dysfunction of INS secretion in β cells may play a role in the progression of T2DM, and if so, improving pancreatic islet β cell function in pre-diabetic stage may be an effective strategy to prevent or treat T2DM. Therefore, we overexpressed SYT7 in *db/db* mice to verify whether it has the effect of alleviating T2DM symptoms. Meanwhile, Trulicity was used as the positive control, and DFO, an iron chelating agent, was used to verify whether reduced iron levels can improve the symptoms of T2DM. SYT7 was successfully overexpressed in β cells of *db/db* mice by in situ injection of AAV8-null or AAV8-SYT7 into the bile duct (Fig. S7A). There was no significant difference in weight between the *db/db* groups after injection, except for a slight increase in AAV8-SYT7 group from 6 weeks (Fig. 6B). All *db/db* mice showed an increasing serum INS level, which was gradually decreased with AAV8-SYT7/Trulicity/DFO treatment after 5 weeks. Noticeably, SYT7 significantly increased serum INS level 1 week after injection and had a better effect in maintaining

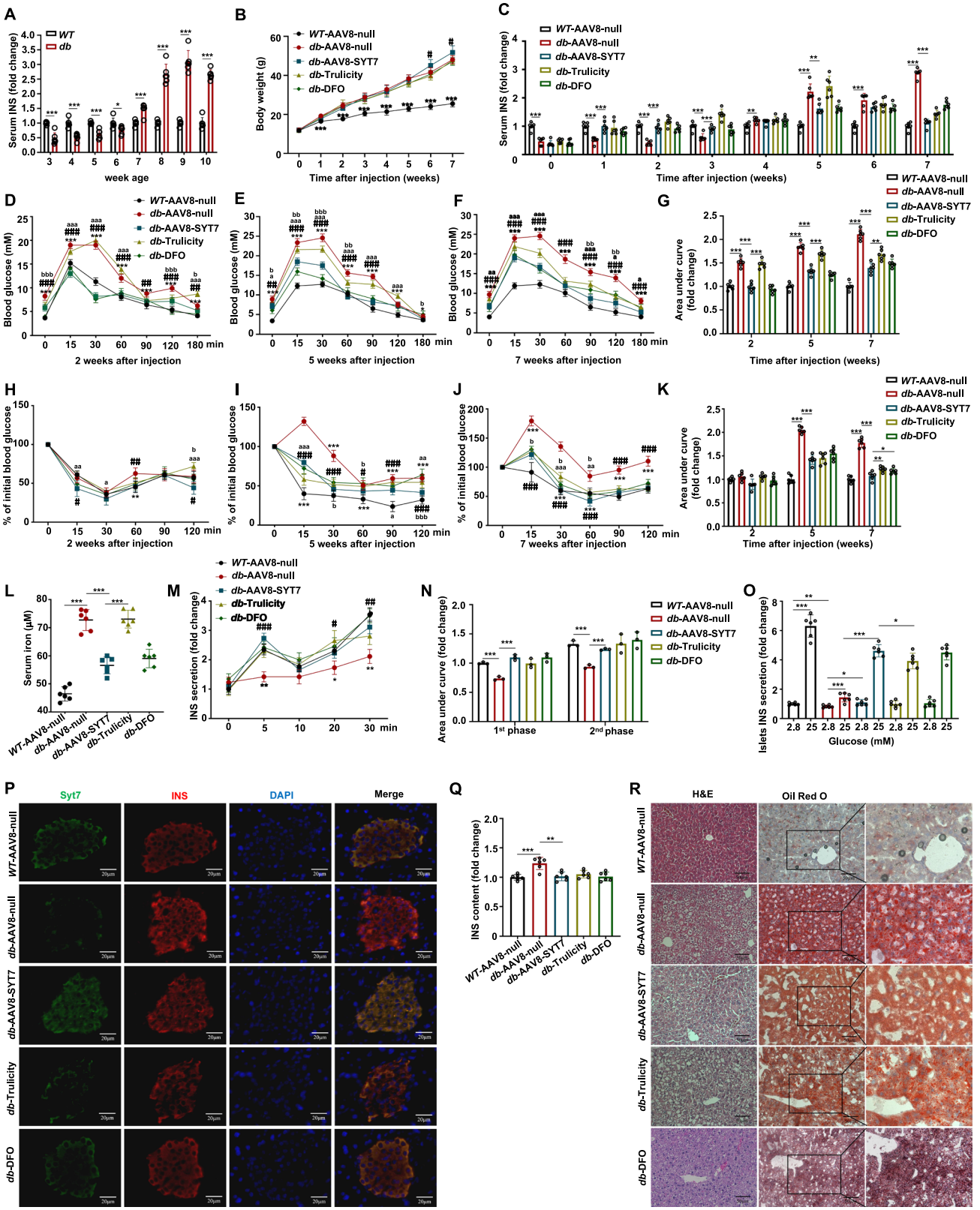
A
WT
db
Serum INS (fold change)
week age
B
WT-AAV8-null
db-AAV8-null
db-AAV8-SYT7
db-Trulicity
db-DFO
Body weight (g)
Time after injection (weeks)
C
Serum INS (fold change)
Time after injection (weeks)
D
Blood glucose (mM)
2 weeks after injection
E
5 weeks after injection
F
7 weeks after injection
G
Area under curve (fold change)
Time after injection (weeks)
H
% of initial blood glucose
2 weeks after injection
I
5 weeks after injection
J
7 weeks after injection
K
Area under curve (fold change)
Time after injection (weeks)
L
Serum iron (μM)
M
INS secretion (fold change)
N
Area under curve (fold change)
1st phase
2nd phase
O
Islets INS secretion (fold change)
Glucose (mM)
P
Syt7
INS
DAPI
Merge
Q
INS content (fold change)
R
H&E
Oil Red O

◂**Fig. 6** Overexpression of SYT7 restored the impaired INS secretion in *db/db* mice. **A** Serum basal INS levels of the WT and *db/db* mice at 3–10 weeks of age. $n=6$ in each cohort. $^{*}P<0.05$, $^{***}P<0.001$. **B** Body weight changes of *db/db* mice after 0–7 weeks of AAV8-SYT7/Trulity/DFO injection. The injection started at the age of 3 weeks, which was recorded as the 0 week after injection. $n=6$ in each cohort. *Indicates the db-AAV8-null group compared with the WT-AAV8-null group, $^{***}P<0.001$. $^{\#}$Indicates that the db-AAV8-SYT7 group was compared with the *db*-AAV8-null group. $^{\#}P<0.05$. **C** The serum basal INS content of *db/db* mice after AAV8-SYT7/Trulity/DFO injection for 0–7 weeks. $n=6$ in each cohort. $^{**}P<0.01$, $^{***}P<0.001$. **D**–**G** After AAV8-SYT7/Trulity/DFO was injected for 2 weeks, 5 weeks and 7 weeks, the results of IPGTT experiment and corresponding AUC. $n=6$ in each cohort. *Indicates the *db*-AAV8-null group compared with the *WT*-AAV8-null group, $^{*}P<0.05$, $^{***}P<0.001$. $^{\#}$Indicates that the *db*-AAV8-SYT7 group was compared with the *db*-AAV8-null group. $^{\#\#}P<0.01$, $^{\#\#\#}P<0.001$. $^{a}$Indicates that the *db*-Trulicity group was compared with the *db*-AAV8-SYT7 group, $^{a}P<0.05$, $^{aa}P<0.01$, $^{aaa}P<0.001$. $^{b}$Indicates that the *db*-DFO group was compared with the *db*-AAV8-SYT7 group, $^{b}P<0.05$, $^{bb}P<0.01$, $^{bbb}P<0.001$. In the comparison of the AUC of each group, $^{**}P<0.01$, $^{***}P<0.001$. **H**–**K** After AAV8-SYT7/Trulity/DFO injection for 2 weeks, 5 weeks and 7 weeks, the results of IPITT experiment and corresponding AUC. $n=6$ in each cohort. *Indicates that the *db*-AAV8-null group compared with the *WT*-AAV8-null group, $^{*}P<0.05$, $^{**}P<0.01$, $^{***}P<0.001$. $^{\#}$Indicates that the *db*-AAV8-SYT7 group was compared with the *db*-AAV8-null group. $^{\#}P<0.05$, $^{\#\#}P<0.01$, $^{\#\#\#}P<0.001$. $^{a}$Indicates that the *db*-Trulicity group was compared with the *db*-AAV8-SYT7 group, $^{a}P<0.05$, $^{aa}P<0.01$, $^{aaa}P<0.001$. $^{b}$Indicates that the *db*-DFO group was compared with the *db*-AAV8-SYT7 group, $^{b}P<0.05$, $^{bbb}P<0.001$. In the comparison of the AUC of each group, $^{*}P<0.05$, $^{**}P<0.01$, $^{***}P<0.001$. **L** Serum iron level of *db/db* mice in each group 3 weeks after AAV8-SYT7/Trucity/DFO injection. $n=6$ in each cohort. $^{***}P<0.001$. **M**, **N** 3 weeks after AAV8-SYT7/Trulicity/DFO injection, the INS biphasic secretion level of *db/db* mice was detected by hyperglycemic clamp test and the AUC was calculated. 0–10 min is defined as the first phase and 10–30 min is defined as the second phase. $n=3$ in each cohort. *Indicates the *db*-AAV8-null group compared with the WT-AAV8-null group, $^{*}P<0.05$, $^{**}P<0.01$. $^{\#}$Indicates the *db*-AAV8-SYT7 group compared with the *db/db*-AAV8-null group, $^{\#}P<0.05$, $^{\#\#}P<0.01$, $^{\#\#\#}P<0.001$. In the comparison of the AUC of each group, $^{***}P<0.001$. **O** The effect of AAV8-SYT7 on GSIS of isolated islets of *db/db* mice was detected by ELISA. $n=5$ in each cohort. $^{*}P<0.05$, $^{**}P<0.01$, $^{***}P<0.001$. **P** 3 weeks after AAV8-SYT7/Trulicity/DFO was injected into *db/db* mice, INS and Syt7 protein levels in β cells were detected by immunofluorescence. Scale bar 20 μm. **Q** The effect of AAV8-SYT7 on the content of INS in islets of *db/db* mice was detected by ELISA. $n=5$ in each cohort. $^{**}P<0.01$, $^{***}P<0.001$. **R** 7 weeks after *db/db* mice were injected with AAV8-SYT7/Trulicity/DFO, the liver tissues were observed by H&E and oil red O staining. Scale bar 50 μm

the INS stationarity (Fig. 6C). Importantly, the IPGTT results showed that blood glucose levels in the AAV8-SYT7 group were lower than that in the Trulicity group at 2 weeks, 5 weeks and 7 weeks after injection (Fig. 6D–G). The IPITT results showed that AAV8-SYT7 could also improve INS sensitivity to a certain extent accordingly (Fig. 6H–K). Interestingly, SYT7 overexpression or DFO treatment significantly downregulated the serum excessive iron levels, by contrast, the Trulicity group had no such effect (Fig. 6L). In vivo and ex vivo experimental results showed that overexpression of SYT7 improved INS secretion after glucose loading (Fig. 6M–O). Immunofluorescence and ELISA results showed increased INS content in islet β cells of *db/db* mice and such increase was restored by the treatment of AAV8-SYT7, Trulicity or DFO (Fig. 6P, Q, Fig. S7B). In addition, since T2DM is usually complicated by fatty liver, the regression of intrahepatic fat can partially indicate an effective control of T2DM [37]. To further confirm the effect of AAV8-SYT7, Trulicity or DFO on *db/db* mice, 7 weeks after injection, mouse liver sections were stained with H&E and oil red O. AAV8-SYT7, Trulicity and DFO treatment all improved the swelling, disordered arrangement and lipid deposition of hepatocytes in *db/db* mice, and AAV8-SYT7 had the best effect (Fig. 6R). In conclusion, our results indicate that overexpression of SYT7 could effectively restore the impaired INS secretion in *db/db* mice and partially improve diabetes symptoms.

## Discussion

This study reveals a novel mechanism for the effect of iron overload on islet β cell dysfunction. We find that excessive iron inhibits INS secretion through suppressing the transcriptional regulation of *SYT7* by OGG1 (Fig. 7). SYT7, a major component of the exocytotic machinery in neurons, is also the major Syt in islet β cells shown to mediate glucose-stimulated INS secretion [38]. Previous studies have clarified that SYT7 functions not only in exocytotic fusion but also in the replenishment of releasable secretory granule (SG) pools in human β cells [38, 39]. However, SYT7's precise expression regulation is still not fully understood. Velde et al. report that CREB is critical for β cell gene expression including *SYT7* via enhancer activation [40]. Human *SYT7* is also discovered to be regulated by TWIST1 in non-small cell lung cancer [41]. In our work, we identify *SYT7* as a new downstream target gene of OGG1 and demonstrate that OGG1/SYT7 axis is essential for INS secretion.

Indeed, OGG1 has long been considered to be an important factor in the metabolic process. *Ogg1*$^{-/-}$ mice exhibit liver and skeletal muscle lipid metabolic disorders and impaired glucose tolerance [10]. OGG1 is of great importance responsible for oxidative DNA damage in rat model of diabetes [42]. Overexpression of OGG1 could protect β cell from free fatty acid-induced apoptosis [43]. However, the exact mechanism of OGG1 in β cells is not clear. In this study, we find that *Ogg1* deletion down-regulated not only *Syt7*, but also the other genes in the *SYTs* family, which suggest that OGG1 may be involved in a wider range of vesicle transport. Further investigation will be necessary to understand how OGG1 regulates *SYTs* expression. Given that the

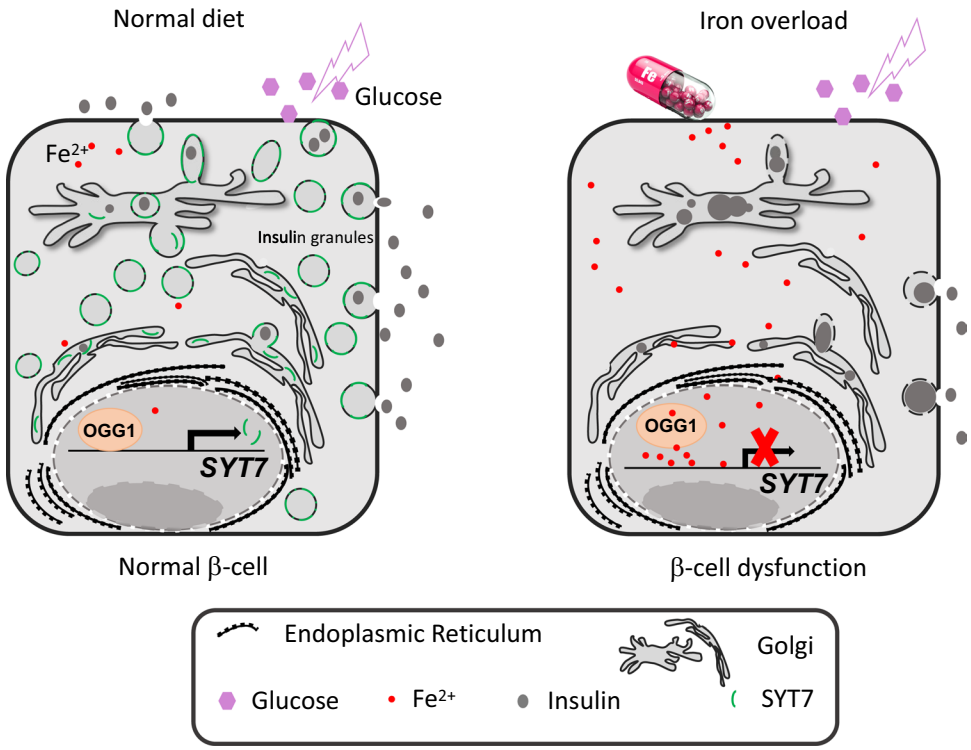


**Fig. 7** Schematic diagram demonstrating INS secretion upon glucose stimulation. Left panel: β cell responds to glucose signal when the $Fe^{2+}$ level is maintained in a constant range. OGG1 binds to *SYT7* promoter and upregulates SYT7 expression, the latter is required for transport vesicles formation and INS secretion. Right panel: excessive iron disrupts the transcriptional regulation of *SYT7* by OGG1, reduces the number of INS transport vesicles, agglomerates INS granules and inhibits INS secretion

neurotransmitter release is the classical function of SYTs family, OGG1/SYT7 axis may also provide insight into a new pathway for neurotransmitter release under oxidative stress.

Interestingly, knockdown of *Ogg1* down-regulated many secretion-related genes, most of which were also down-regulated with $FeSO_4$ treatment (Fig. S8). Our data show that OGG1 positively regulates *SYT7* transcription, however, *db/db* mice and β-DKO (*Swi/Snf* deficiency leads to dysfunction) mice exhibit negative correlation between *Ogg1* and *Syt7*. Excessive iron may be appropriate to explain this contradictory phenomenon. It has been established that ROS levels are increased in diabetic mice [44], as the key factor responding to oxidative stress, OGG1 is increased accordingly, but *SYT7* could not be effectively up-regulated by OGG1 even if there are a large amount of OGG1 in cells, because excessive iron perturbs this regulation. Similarly, in our iron overload model, excessive iron increases intracellular ROS and Ogg1 levels, while inhibits *Syt7* expression.

Such mechanism of action of iron also applies to HFD model. We isolated the serum of long-term (more than 6 months) HFD mice and found that the serum $Fe^{2+}$ level was significantly increased (Fig. S9). Cheng et al. show that the use of iron chelation deferoxamine (DFO) improved the expression of genes related to glucose transport and glycolysis in HFD mouse and human islets, and also improve INS secretion capacity [29]. Together, iron plays a key role in occurrence and development of diabetes. However, the application of iron chelation therapy in the treatment of diabetes is controversial [45]. Therefore, finding the exact downstream pathway of iron is important for the treatment of diabetes.

After confirming that SYT7 is the downstream effector mediating excessive iron-induced β cell dysfunction, we thus investigated the efficacy of AAV8-SYT7 in the treatment of T2DM. As expected, AAV8-SYT7 effectively improves impaired glucose tolerance, alleviated IR, and improves liver lipid deposition. Importantly, blood INS level fluctuates less compared with GLP-1RA (Fig. 6C), which indicates that SYT7 overexpression has an advantage in controlling the stability of blood glucose. H&E staining shows that there is no damage to major organs by AAV8-SYT7 (Fig. S5B). Importantly, our data showed that the use of iron chelating agent or AAV8-SYT7 effectively improved IR, which suggests that iron clearance or SYT7 overexpression increases the sensitivity of target tissues to INS. However, whether this increase is an indirect feedback caused by reduced glucose toxicity or a direct effect of increased INS utilization due to improved INS release still requires further exploration. In conclusion, our study suggests that AAV8-SYT7 is a valuable treatment modality for T2DM. Notwithstanding, there are still many issues that need to be considered. First, AAV8-SYT7 may be effective in patients diagnosed at early stage, because those with a long history of T2DM are usually associated with progressive β cell loss. Second, our data show that SYT7 overexpression in *db/db* mice increases weight to a certain extent, which may be due to the increased availability of INS. Therefore, for those obese

diabetic patients, SYT7 overexpression combined with weight loss strategies may be necessary. Considering the effects of off-target, immunogenicity and other issues of AAV vectors [46–48], exploring safer ways to overexpress or phosphorylate SYT7 may be a new idea for the treatment of T2DM [49].

**Supplementary Information** The online version contains supplementary material available at https://doi.org/10.1007/s00018-023-04802-y.

**Acknowledgements** We thank the scholars for their selfless help in this research. Dr. Rufeng Xu, Dr. Yunxia Zhu, and Prof. Xiao Han from Nanjing Medical University instructed the intraductal virus infusion. Prof. Wei Yu and Huicong Zhou from Taikang Xianlin Drum Tower Hospital helped to detect serum $Fe^{2+}$. Prof. Xueqing Ba from Northeast Normal University provided the OGG1 overexpression plasmid. Dr. Lei Lan and Prof. Long Chen from Nanjing Normal University provided ultra-thin sectioning equipment. Dr. Jian Liu from Nanjing Normal University provided assistance with the experimental method. Dr. Lili Gu from Nanjing Normal University for answering the clinical questions.

**Author contributions** XZ and FP designed the study. XZ and YM obtained the data. MS, JX, SC and ZH contributed to and supervised the in vivo experimentation. MH and LH helped with the imaging analysis. MC and TJ provided support for the collection of outpatient cases. ZG provided funding support and support for communication with the administrative department. XZ drafted the manuscript. FP provided support for cooperation with the technology platform and manuscript revision. All authors reviewed and approved the manuscript. FP and ZG are the guarantors of this work and, as such, had full access to all of the data in the study and take responsibility for the integrity of the data and the accuracy of the data analysis.

**Funding** This work was supported by National Natural Science Foundation of China (81872284, 32171407) and Jiangsu Graduate Research and Practice Innovation Program (KYCX20-1187).

**Availability of data and materials** All data associated with this study are present in the paper or Supplementary Materials.

## Declarations

**Conflict of interest** The authors declare that they have no competing interests.

## References

1. Holman RR (2013) Optimal management of T2DM remains elusive. Nat Rev Endocrinol 9(2):67–68
2. Chen L, Magliano DJ, Zimmet PZ (2011) The worldwide epidemiology of type 2 diabetes mellitus-present and future perspectives. Nat Rev Endocrinol 8(4):228–236
3. Simcox JA, McClain DA (2013) Iron and diabetes risk. Cell Metab 17(3):329–341
4. Zhang R, Huang X, Li Y, Yu Z, Wu Y, Zha B, Ding H, Zang S, Liu J (2021) Serum ferritin as a risk factor for type 2 diabetes mellitus, regulated by liver transferrin receptor 2. Endocr Connect 10(12):1513–1521
5. Azevedo-Martins AK, Lortz S, Lenzen S, Curi R, Eizirik DL, Tiedge M (2003) Improvement of the mitochondrial antioxidant defense status prevents cytokine-induced nuclear factor-κB activation in insulin-producing cells. Diabetes 52(1):93–101
6. David SS, O'Shea VL, Kundu S (2007) Base-excision repair of oxidative DNA damage. Nature 447(7147):941–950
7. Mao G, Pan X, Zhu BB, Zhang Y, Yuan F, Huang J, Lovell MA, Lee MP, Markesbery WR, Li GM, Gu L (2007) Identification and characterization of OGG1 mutations in patients with Alzheimer's disease. Nucl Acids Res 35(8):2759–2766
8. Gönül N, Kadioglu E, Kocabaş NA, Özkaya M, Karakaya AE, Karahalil B (2012) The role of GSTM1, GSTT1, GSTP1, and OGG1 polymorphisms in type 2 diabetes mellitus risk: a case–control study in a Turkish population. Gene 505(1):121–127
9. Tyrberg B, Anachkov KA, Dib SA, Wang-Rodriguez J, Yoon KH, Levine F (2002) Islet expression of the DNA repair enzyme 8-oxoguanosine DNA glycosylase (Ogg1) in human type 2 diabetes. BMC Endocr Disord 2(1):1–10
10. Sampath H, Vartanian V, Rollins MR, Sakumi K, Nakabeppu Y, Lloyd RS (2012) 8-Oxoguanine DNA glycosylase (OGG1) deficiency increases susceptibility to obesity and metabolic dysfunction. PLoS ONE 7(12):e51697
11. Ba X, Bacsi A, Luo J, Aguilera-Aguirre L, Zeng X, Radak Z, Brasier AR, Boldogh I (2014) 8-oxoguanine DNA glycosylase-1 augments proinflammatory gene expression by facilitating the recruitment of site-specific transcription factors. J Immunol 192(5):2384–2394
12. Boldogh I, Hajas G, Aguilera-Aguirre L, Hegde ML, Radak Z, Bacsi A, Sur S, Hazra TK, Mitra S (2012) Activation of ras signaling pathway by 8-oxoguanine DNA glycosylase bound to its excision product, 8-oxoguanine. J Bio Chem 287(25):20769–20773
13. Fleming AM, Ding Y, Burrows CJ (2017) Oxidative DNA damage is epigenetic by regulating gene transcription via base excision repair. Proc Natl Acad Sci USA 114(10):2604–2609
14. Wang W, Ma Y, Huang M, Liang W, Zhao X, Li Q, Wang S, Hu Z, He L, Gao T, Chen J, Pan F, Guo Z (2021) Asymmetrical arginine dimethylation of histone H4 by 8-oxoG/OGG1/PRMT1 is essential for oxidative stress-induced transcription activation. Free Radic Bio Med 164:175–186
15. Xiao X, Guo P, Prasadan K, Shiota C, Peirish L, Fischbach S, Song Z, Gaffar I, Wiersch J, El-Gohary Y, Husain SZ, Gittes GK (2014) Pancreatic cell tracing, lineage tagging and targeted genetic manipulations in multiple cell types using pancreatic ductal infusion of adeno-associated viral vectors and/or cell-tagging dyes. Nat Protoc 9(12):2719–2724
16. Zhu YX, Zhou YC, Zhang Y, Sun P, Chang XA, Han X (2021) Protocol for in vivo and ex vivo assessments of glucose-stimulated insulin secretion in mouse islet β cells. STAR Protoc 2(3):100728
17. Zhu Y, Shu T, Lin Y, Wang H, Yang J, Shi Y, Han X (2011) Inhibition of the receptor for advanced glycation end products (RAGE) protects pancreatic β-cells. Biochem Bioph Res Co 404(1):159–165
18. Huang Q, You W, Li Y, Sun Y, Zhou Y, Zhang Y, Liu D, Zhan S, Zhu Y, Han X (2018) Glucolipotoxicity-inhibited miR-299-5p regulates pancreatic β-cell function and survival. Diabetes 67(11):2280–2292
19. Ci S, Xia W, Liang W, Qin L, Zhang Y, Dianov GL, Wang M, Zhao X, Wu C, Alagamuthu KK, Hu Z, He L, Pan F, Guo Z (2020) Src-mediated phosphorylation of GAPDH regulates its nuclear localization and cellular response to DNA damage. FASEB J 34(8):10443–10461
20. Marku A, Galli A, Marciani P, Dule N, Perego C, Castagna M (2021) Iron metabolism in pancreatic beta-cell function and dysfunction. Cells 10(11):2841
21. Sampath H, Lloyd RS (2019) Roles of OGG1 in transcriptional regulation and maintenance of metabolic homeostasis. DNA Repair 81:102667

22. Gustavsson N, Lao Y, Maximov A, Chuang JC, Kostromina E, Repa JJ, Li C, Radda GK, Südhof TC, Han W (2008) Impaired insulin secretion and glucose intolerance in synaptotagmin-7 null mutant mice. Proc Natl Acad Sci USA 105(10):3992–3997
23. Pang ZP, Südhof TC (2010) Cell biology of $Ca^{2+}$-triggered exocytosis. Curr Opin Cell Biol 22(4):496–505
24. Gerber SH, Südhof TC (2002) Molecular determinants of regulated exocytosis. Diabetes 51(suppl 1):S3–S11
25. Gandini MA, Sandoval A, González-Ramírez R, Mori Y, de Waard M, Felix R (2011) Functional coupling of Rab3-interacting molecule 1 (RIM1) and L-type Ca2+ channels in insulin release. J Bio Chem 286(18):15757–15765
26. Kwan EP, Xie L, Sheu L, Nolan CJ, Prentki M, Betz A, Brose N, Gaisano HY (2006) Munc13-1 deficiency reduces insulin secretion and causes abnormal glucose tolerance. Diabetes 55(5):1421–1429
27. Yasuda T, Shibasaki T, Minami K, Takahashi H, Mizoguchi A, Uriu Y, Numata T, Mori Y, Miyazaki J, Miki T, Seino S (2010) Rim2α determines docking and priming states in insulin granule exocytosis. Cell Metab 12(2):117–129
28. Zhang W, Efanov A, Yang SN, Fried G, Kölare S, Brown H, Zaitsev S, Berggren PO, Meister B (2000) Munc-18 associates with syntaxin and serves as a negative regulator of exocytosis in the pancreatic β-cell. J Bio Chem 275(52):41521–41527
29. Cheng K, Ho K, Stokes R, Scott C, Lau SM, Hawthorne WJ, O'Connell PJ, Loudovaris T, Kay TW, Kulkarni RN, Okada T, Wang XL, Yim SH, Shah Y, Shane TG, Biankin AV, Kench JG, Laybutt DR, Gonzalez FJ, Kahn CR, Gunton JE (2010) Hypoxia-inducible factor-1α regulates β cell function in mouse and human islets. J Clin Invest 120(6):2171–2183
30. Marquez R, Hettler F, Hausinger R, Schreck C, Landspersky T, Henkel L, Angerpointner C, Demir IE, Schiemann M, Bassermann F, Götze KS, Istvánffy R, Oostendorp RA (2021) Secreted factors from mouse embryonic fibroblasts maintain repopulating function of single cultured hematopoietic stem cells. Haematologica 106(10):2633
31. Moghadam PK, Jackson MB (2013) The functional significance of synaptotagmin diversity in neuroendocrine secretion. Front Endocrinol 4:124
32. Wang R, Hao W, Pan L, Boldogh I, Ba X (2018) The roles of base excision repair enzyme OGG1 in gene expression. Cell Mol Life Sci 75(20):3741–3750
33. Zharkov DO, Rosenquist TA (2002) Inactivation of mammalian 8-oxoguanine-DNA glycosylase by cadmium (II): implications for cadmium genotoxicity. DNA Repair 1(8):661–670
34. Ashcroft FM, Rorsman P (2012) Diabetes mellitus and the β cell: the last ten years. Cell 148(6):1160–1171
35. Fonseca VA (2009) Defining and characterizing the progression of type 2 diabetes. Diabetes Care 32(suppl 2):S151–S156
36. Altamura S, Kopf S, Schmidt J, Müdder K, da Silva AR, Nawroth P, Muckenthaler MU (2017) Uncoupled iron homeostasis in type 2 diabetes mellitus. J Mol Med (Berl) 95(12):1387–1398
37. Williams KH, Shackel NA, Gorrell MD, McLennan SV, Twigg SM (2013) Diabetes and nonalcoholic fatty liver disease: a pathogenic duo. Endocr Rev 34(1):84–129
38. Dolai S, Xie L, Zhu D, Liang T, Qin T, Xie H, Kang Y, Chapman ER, Gaisano HY (2016) Synaptotagmin-7 functions to replenish insulin granules for exocytosis in human islet β-cells. Diabetes 65(7):1962–1976
39. Rorsman P, Braun M (2013) Regulation of insulin secretion in human pancreatic islets. Annu Rev Physiol 75:155–179
40. Van de Velde S, Wiater E, Tran M, Hwang Y, Cole PA, Montminy M (2019) CREB promotes beta cell gene expression by targeting its coactivators to tissue-specific enhancers. Mol Cell Biol 39(17):e00200-e219
41. Liu X, Li C, Yang Y, Liu X, Li R, Zhang M, Yin Y, Qu Y (2019) Synaptotagmin7 in twist-related protein 1-mediated epithelial-Mesenchymal transition of non-small cell lung cancer. EBioMedicine 46:42–53
42. Simone S, Gorin Y, Velagapudi C, Abboud HE, Habib SL (2008) Mechanism of oxidative DNA damage in diabetes: tuberin inactivation and downregulation of DNA repair enzyme 8-oxo-7, 8- dihydro-2'-deoxyguanosine-DNA glycosylase. Diabetes 57(10):2626–2636
43. Rachek LI, Thornley NP, Grishko VI, LeDoux SP, Wilson GL (2006) Protection of INS-1 cells from free fatty acid-induced apoptosis by targeting hOGG1 to mitochondria. Diabetes 55(4):1022–1028
44. Kaneto H, Katakami N, Matsuhisa M, Matsuoka TA (2010) Role of reactive oxygen species in the progression of type 2 diabetes and atherosclerosis. Mediat Inflamm 2010:453892
45. Gamberini MR, De Sanctis V, Gilli G (2008) Hypogonadism, diabetes mellitus, hypothyroidism, hypoparathyroidism: incidence and prevalence related to iron overload and chelation therapy in patients with thalassaemia major followed from 1980 to 2007 in the Ferrara Centre. Pediatr Endocr Rev Proc 6:158–169
46. Haery L, Deverman BE, Matho KS, Cetin A, Woodard K, Cepko C, Guerin KI, Rego MA, Ersing I, Bachle SM, Kamens J, Fan M (2019) Adeno-associated virus technologies and methods for targeted neuronal manipulation. Front Neuroanat 13:93
47. Zhou C, Sun Y, Yan R, Liu Y, Zuo E, Gu C, Han L, Wei Y, Hu X, Zeng R, Li Y, Zhou H, Guo F, Yang H (2019) Off-target RNA mutation induced by DNA base editing and its elimination by mutagenesis. Nature 571(7764):275–278
48. Ronzitti G, Gross DA, Mingozzi F (2020) Human immune responses to adeno-associated virus (AAV) vectors. Front Immunol 11:670
49. Wu B, Wei S, Petersen N, Ali Y, Wang X, Bacaj T, Rorsman P, Hong W, Südhof TC, Han W (2015) Synaptotagmin-7 phosphorylation mediates GLP-1-dependent potentiation of insulin secretion from β-cells. Proc Natl Acad Sci USA 112(32):9996–10001